Preprints.org

Article

Not peer-reviewed version

Enhancement of Database NORAD-Atomic-Data for Atomic Processes in Plasma

Sultana N. Nahar * and Guillermo Hinojosa-Aquirre

Posted Date: 15 December 2023

doi: 10.20944/preprints202312.1161.v1

Keywords: Atomic data; transition probabilities; photoionization cross sections; electron-ion recombination cross sections and rate coefficients; lifetimes; electron-impact excitation; Line ratios; third generation synchrotron radiation

Preprints.org is a free multidiscipline platform providing preprint service that is dedicated to making early versions of research outputs permanently available and citable. Preprints posted at Preprints.org appear in Web of Science, Crossref, Google Scholar, Scilit, Europe PMC.

Copyright: This is an open access article distributed under the Creative Commons Attribution License which permits unrestricted use, distribution, and reproduction in any medium, provided the original work is properly cited.

Preprints (www.preprints.org) | NOT PEER-REVIEWED | Posted: 15 December 2023 doi:10.20944/preprints202312.1161.v1

Disclaimer/Publisher's Note: The statements, opinions, and data contained in all publications are solely those of the individual author(s) and contributor(s) and not of MDPI and/or the editor(s). MDPI and/or the editor(s) disclaim responsibility for any injury to people or property resulting from any ideas, methods, instructions, or products referred to in the content.

Article

Enhancement of Database NORAD-Atomic-Data for Atomic Processes in Plasma

Sultana N. Nahar [1,*,†] and Guillermo Hinojosa-Aguirre [2,†]

[1] Department of Astronomy, The Ohio State University, Columbus, OH 43210, USA
[2] Universidad Nacional Autónoma de México, Instituto de Ciencias Físicas, A. P. 48-3, Cuernavaca 62251, Mexico
* Correspondence: nahar.1@osu.edu; Tel.: 1-614-292-1888
† Both authors contributed equally to this work.

Abstract: We report recent enhancements of the online atomic database at the Ohio State University, NORAD-Atomic-Data, that provides various parameters for radiative and collisional atomic processes dominant in astrophysical plasma. NORAD stands for Nahar Osu RADiative. The database belongs to the data sources, especially for the latest works, of the international collaborations of the Opacity Project and the Iron Project. The contents of the database are calculated values for energies, oscillator strengths, radiative decay rates, lifetimes, cross sections for photoionization, electron-ion recombination cross sections and recombination rate coefficients. We have recently expanded NORAD-Atomic-Data with several enhancements over those reported earlier. They are as follows. i) We continue to add energy levels, transition parameters, cross sections for atoms and ions with their publications. ii) Recently added radiative atomic data contains significant amount of transition data for photo-absorption spectral features corresponding to x-ray resonance fluorescence effect, prominent wavelength regions of bio-signature elements, such as phosphorus ions, and emission bumps of heavy elements, such as of lanthanides, that may be created in a kilonova event. We are including iii) collisional data for electron-impact-excitation, iv) experimental data for energies and oscillator strengths for line formation, v) experimental cross sections for photoionization that can be applied for benchmarking and other applications, and vi) introduction of a web-based interactive feature to calculate spectral line ratios at various plasma temperature and density diagnostics, starting with our recently published data for P II. We presented summary description of theoretical backgrounds for the computed data in the earlier paper. With introduction of experimental results, we present summary description of measurement of high resolution photoionization cross sections at Advanced Light Source of LBNL synchrotron set-up and briefly discuss other set-ups. These additions should make NORAD-Atomic-Data more versatile for various applications. For brevity, we provide information on the extensions and avoid repetition of data description of the original paper.

Keywords: atomic data; transition probabilities; photoionization cross sections; electron-ion recombination cross sections and rate coefficients; lifetimes; electron-impact excitation; Line ratios; third generation synchrotron radiation

1. Introduction: NORAD-Atomic-Data

The atomic database, NORAD-Atomic-Data [1,2], contains parameters of atomic processes, as described below, that are dominant in astrophysical plasma. A major part of the data were obtained under the two international collaborations of the Opacity Project (OP) [3,4] and the Iron Project (IP) [5], and constitute the atomic data source, either for new data or revised and more expanded data for the OP and the IP.

The author (SNN) is the leading member of the Opacity Project ([4]) and the Iron Project (IP [5]) for studying the radiative atomic processes and has been computing extensive sets of radiative data. To meet the need of astronomers accessing atomic data all time from an independent platform the online database NORAD-Atomic-Data [1,2] was founded in 2007 at the Ohio State University.

© 2023 by the author(s). Distributed under a Creative Commons CC BY license.

Preprints (www.preprints.org) | NOT PEER-REVIEWED | Posted: 15 December 2023 doi:10.20944/preprints202312.1161.v1

NORAD-Atomic-Data provides data which are not available or which are updated with larger wavefunction expansion and higher accuracy than those in the two atomic databases, TOPbase [7] founded under the OP and TIPbase [8] founded under the IP. All data are processed for clarity and easy applications before uploading them to NORAD-Atomic-Data as explained in [1]. This report presents several recently added enhancements and under development in the latest form of the database.

Details of format and data structure, and summary of theoretical background, accuracy estimation of data for the processes have been described in Nahar [1]. More detailed theoretical background are available from Pradhan and Nahar in textbook "Atomic Astrophysics and Spectroscopy" [9] which is a culmination of findings in atomic processes revealed in the study under the OP and IP. Here we present summary outlines for experimental methods, and more details of one particular experimental method with Advanced Light Source (ALS) at Lawrence Berkeley National Laboratory (LBNL) synchrotron for measurement of high-resolution photoionization cross sections.

We provide below outlines for general guidance on the atomic processes in plasma and relevant contents of the database.

2. Atomic Processes and Parameters in NORAD-Atomic-Data

There are four atomic process that occur commonly in astrophysical plasma - photo-excitation,photoionization, electron-ion recombination, electron-impact excitation. Study of an atomic process requires wavefunctions and energy levels of the atomic system being studied to calculate various parameters of the processes. These parameters at database NORAD-Atomic-Data have been computed using energy levels and wavefunctions generated either by the R-matrix method using its package of and associated codes [10–13] or by central-field approximation using atomic structure code SUPERSTRUCTURE (SS) [14,15]. Followings are the atomic processes and associated data files.

i) Energy levels:

NORAD-Atomic-Data provides energy table for each atomic species for which atomic processes have been studied. Although basically the same, there are some differences in representations between the energies obtained from the R-matrix method and from atomic structure calculations.

The R-matrix method calculates absolute values for the energy levels and can show the clear presence of ionization threshold as negative energies for bound levels turn positive for continuum levels when energies reach to the threshold. This option is enabled in the R-matrix codes for nonrelativistic LS coupling approximation [10]. The latest version of the relativistic Breit-Pauli R-matrix (BPRM) codes [13] computes only the bound levels, that is, no positive energies are computed. In contrast to R-matrix, SS computes energy values relative to the ground level which is set to zero, and hence show positive values. This representation is the same as that of for energies compiled and available at the website of the National Institute of Standards and Technology (NIST [16]). Atomic structure calculations, such as of SS, do not determine the ionization threshold and computes all energy levels belonging to the set of configurations provided. Hence the computed energies can continue from bound to beyond the ionization threshold. NIST provides ionization thresholds obtained separately.

Energy levels computed in the R-matrix method [10,13] go from ground level to highly excited levels with $n \leq 10$, $l \leq 9$, and of parities even and odd, and hence correspond to a large set of levels. The number of energy levels from SS [14,15] is typically less since the excitation goes up to $n \leq$ 4-6 although it includes all possible combination of quantum numbers.

R-matrix computations include all quantities, such as, oscillator strengths, photoionization cross sections, electron-ion recombination rate coefficients for all levels going up to n=10. SS computes all transition parameters for levels going up to the highest orbitals with n=4-6.

Formats for the energy files are described in [1].

ii) Radiative atomic transition of excitation and de-excitation:

Preprints (www.preprints.org) | NOT PEER-REVIEWED | Posted: 15 December 2023 doi:10.20944/preprints202312.1161.v1

$$X^{+q} + h\nu \rightleftharpoons X^{+q*} \tag{1}$$

X^{+q} is the ion X of charge q and asterisk indicates excitation. The parameters of interest are: i) Line strength (S), ii) Oscillator strength (f), iii) Radiative decay rate (A-value), for the transitions and iv) Lifetimes (τ) of levels.

Radiative data for bound-bound transitions are of the following types: allowed electric dipole (E1) of the same spin (for LS-allowed and fine structure) and different (intercombination) spin multiplicities of the final state from the initial one, electric quadrupole (E2), electric octupole (E3), magnetic dipole (M1), and magnetic quadrupole (M2). Details of these are described in [9] For many ions at the database, E1 transitions have been obtained from using BPRM method while parameters for forbidden transitions have been obtained from Breit-Pauli atomic structure calculations using code SS. When R-matrix method has not been used, E1 transitions obtained using SS are presented. Individual transitions form spectral lines. However data for large number of transitions are needed to determine the opacity in plasma, creation of synthetic spectrum of ions, etc.

Formats for the transition parameters are described in [1].

iii) Photoionization (PI):

The process proceeds directly by photoabsorption as

$$X^{+q} + h\nu \rightarrow X^{+q+1} + e \tag{2}$$

which produces smooth photoionization cross section (σ_{PI}) feature, such as the background σ_{PI}. Photoionization can occur indirectly via formation of an intermediate doubly-excited autoionizing state before ionization as

$$h\nu + X^{+q} \rightleftharpoons (X^{+q})^{**} \rightleftharpoons X^{+q+1} + e \tag{3}$$

This takes place when the photon energy matches to that of a Rydberg state and introduces a resonance, known as a Rydberg resonance, in the cross section σ_{PI}. A resonance has considerable impact, not only by its magnitude of very high probability, but also on the shape of the background cross section. In addition to Rydberg series of resonances, Seaton resonance also forms when the core ion goes through a dipole allowed transition before breaking down for photoionization.

Central-field approximation, such as, distorted wave, can produce only the background cross sections, not the resonances. Only the close-coupling (CC) approximation using the R-matrix method can produce resonances automatically along with background cross sections. We use relativistic Breit-Pauli R-matrix (BPRM) codes [13,17] with CC wavefunction expansion to compute σ_{PI}. The resonances are treated with radiation damping effect [18] for precise treatment. However, we also use nonrelativistic R-matrix codes [10] when relativistic fine structure calculations become computationally prohibitive.

The parameters calculated for photoionization are cross sections for all bound levels from ground to $n \leq 10$. They are usually of two types. i) Partial cross section for photoionization $\sigma_{PI}(g, E)$ leaving the core ion in its ground level and ii) total cross section for photoionization σ_{PI} leaving the core ion in the ground and various excited states as the photon energy crosses the excitation thresholds. Total cross section is the sum of all partial cross sections for leaving the core ion in various states. iii) We also calculate the individual partial cross sections leaving the core ion in various excited levels. However, such partials are saved only for the ground level for which these cross sections have more applications.

Formats for photoionization cross sections are described in [1]

iv) Electron-ion recombination:

Preprints (www.preprints.org) | NOT PEER-REVIEWED | Posted: 15 December 2023 doi:10.20944/preprints202312.1161.v1

It is the inverse process of photoionization where electron-ion can recombine directly, known as radiative recombination (RR), as

$$X^{+q+1} + e \rightarrow X^{+q} + h\nu, \tag{4}$$

This provides the smooth background feature of recombination cross section. Recombination can also occur through an intermediate recombination (DR), as

$$e + X^{+q} \rightleftharpoons (X^{+q-1})^{**} \rightleftharpoons \begin{cases} e + X^{+q} & \text{AI} \\ X^{+q-1} + h\nu & \text{DR} \end{cases} \tag{5}$$

The intermediate autoionizing state can lead to autoionization (AI) where the electron goes free, or to radiative decay channel of DR by emission of a photon.

For electron-ion recombination, we calculate the atomic parameters using the unified method of Nahar and Pradhan [17,19] for: i) Level-specific total recombination (includes both RR and DR) rate coefficients ($\alpha_{RC}(i)$) of all bound levels going up to $n \leq 10$, ii) total recombination rate coefficient with respect to temperature $\alpha_{RC}(T)$) which is the summed contributions of all levels with $n \leq 10$ and of levels with $10 < n \leq \infty$ obtained using extension of Bell and Seaton theory [17,20] on DR, iii) total recombination cross sections ($\sigma_{RC}(E)$) and iv) total recombination rate coefficient ($\alpha_{RC}(E)$) with respect to photo-electron energy E. Recombination resonances can be seen in emission spectra as dielectronic recombination (DES) lines and total $\alpha_{RC}(T)$ is used in determination of ionization fractions in photoionized or collisional plasma. Data format is explained in [1].

v) Electron-impact excitation (EIE):

Electron impact excitation of a target leads to emission of a photon as the excited electron drops down:

$$e + X^{+Z} \rightarrow e' + X^{+Z*} \rightarrow X^{+Z} + h\nu + e' \tag{6}$$

The line of the emitted photon carries information of the process. Similar to photoionization, an autoionizing state that introduces a resonance can form if the impact energy equals to that of a Rydberg state. EIE parameters are: i) Collision strength (Ω), ii) Effective collision strengths (γ), iii) Collision rate coefficients (q_{ij}). Emission lines from levels excited by EIE provides diagnostics of thin plasma. Details can be found in, e.g., [9].

3. Merged Beam Technique at the Advanced Light Source at the Lawrence Berkeley National Laboratory

For a general concept of measurement of photoionization cross sections, we provide summary description of the experimental set-up that was installed at the Advanced Light Source (ALS) Synchrotron Facility at the LBNL. This is one most accurate experimental set-up with third generation synchrotron radiation for high-resolution photoionization cross section.

For a review about the merged beam technique (MBT), we refer to the article by Phaneuf *et al.* [21]. For more information about synchrotron technology we refer to the article by Margaritondo [22]. For a detailed description of this experimental set-up, we refer to references [23,24]. Here, we present a brief but complete description of the method.

To implement the experimental realization of photoionization Eqs. (2,3), an ion beam and a photon beam are merged. Also, parameters, such as, their width, intensity and overlap length have to be measured.

3.1. The Photon Beam

The experimental set-up was located at the ALS, a third-generation synchrotron accelerator at the LBNL. The Merged Beam Technique (MBT) was implemented in one of the end-lines of the synchrotron ring (beam line 10.0.1.). The end-station was intended to be a multi-user experiment.

Preprints (www.preprints.org) | NOT PEER-REVIEWED | Posted: 15 December 2023 doi:10.20944/preprints202312.1161.v1

This MBT end-station was decommissioned in 2015 and by the end of the MBT operational time, the synchrotron's electron's storage-ring operated with 500 mA current at 1.9 GeV in *top-off* mode, *i. e.*, with a quasi-continuous injection of electrons that results in a constant current and stability improvement.

The photon-beam was generated by a 10 cm period undulator inserted in the electron's trajectory inside the synchrotron's ring. As a result, the relativistic electrons oscillate producing a photon-beam with a width less than 1 mm and with a divergence less than 0.05°. This photon-beam was then directed to shine over a grazing spherical-grating monochromator, producing wavelength separation as a function of the grazing angle. In this manner, it was possible to scan the photon energy by rotating the grating. Also, the exit slit of the monochromator and the undulator gap were adjusted to maximize the photon-beam intensity.

A calibrated silicon photodiode [25] with a 5% uncertainty was used to measure the photon flux. This diode generated a current that was read by a precision current meter that provided a normalization signal to the data acquisition system. Collisions of the X^{q+} ions with the residual gas in the vacuum system may generate $X^{(q+1)+}$ signal. To separate this background signal from the actual photoionization signal, the photon-beam was mechanically pulsed using a controlled chopper-wheel to produce a signal correlated to photons and a signal correlated only to background $X^{(q+s)+}$, and in turn subtract it from the signal generated when the photons were on. s is the order of photoionization. For instance, $s = 1$ corresponds to single photoionization.

The energy resolution of the photon-beam was typically between 10 meV and 40 meV and it was to nominally programmed on the control system to later derive a more realistic value from FWHM (full width half maximum) of resonance peaks. The energy of the photon beam was nominally set by the control interface system associated to the beam line. The energy calibration was further improved with the aid of an ionization gas-cell located on a side branch of the experimental set-up, in this cell He [26] and Kr [27] gases were injected. Their ionization spectra were used as a reference in the energy interval from 21.218 eV to 63.355 eV. Estimates of the energy error from this technique, varied from about $\pm$ 30 meV to $\pm$ 10 meV, depending on different author's implementations. For instance, this calibration was employed for the single photoionization spectrum measurement of Cl^+ [28] resulting in an agreement with NIST database [29] up to three decimal digits (in eV).

Although, the photon flux and resolution of this facility were uniquely fitted to measure photoionization, higher-order harmonic components in the photon beam, especially in the lower energy interval of its operational range (17 eV to 80 eV) can have considerable effects. This issue was assessed in references [23,25,30].

3.2. The Ion Beam

To generate the ion beam, an initial stage to create the ions was implemented by installing an ion-source. Different types of ion sources were positioned in the end-station. For instance, an ECR (electron cyclotron resonance) ion source was used to generate multicharged ion beams. For example C^{2+}, N^{3+} and O^{4+} [31]. In the initial stage of the experiment, a hot-filament ion-source was used to generate O^+ [32] and Ne^+ [33] ions; a caesium-sputter ion source was used for Na^- [34] and a plasma emission source to produce Li^+ ions [35].

The ion source was mounted on a floated voltage circuit, in a way, that the whole ion source was biased to the acceleration voltage. As a consequence, ions generated inside the ion source were repelled or extracted by Coulomb repulsion. The standard repulsion voltage was 5 kV or 6 kV to produce ion beams of energies of the order of keV because at these energies, the ionization by collision with the residual gas is expected to be low.

X^{q+} ions extracted from the ion source were accelerated toward a cylindrical electrostatic lens set that provided focusing to the ions. Following, the ions were selected by mass-to-charged analysis with a 60° sector magnet. It is necessary to have fine control of the ion beam direction, for this purpose, sets of electric fields perpendicular to the ion beam trajectory were implemented by applying small voltages to steering plate electrodes (not shown in Figure 1) located at the entrance and the exit of a

Preprints (www.preprints.org) | NOT PEER-REVIEWED | Posted: 15 December 2023 doi:10.20944/preprints202312.1161.v1

deflector made of two spherical-sector electrodes. This deflector produced a 90° change in the ion beam trajectory for the ion beam to face the counter-propagating photon beam from the ALS.

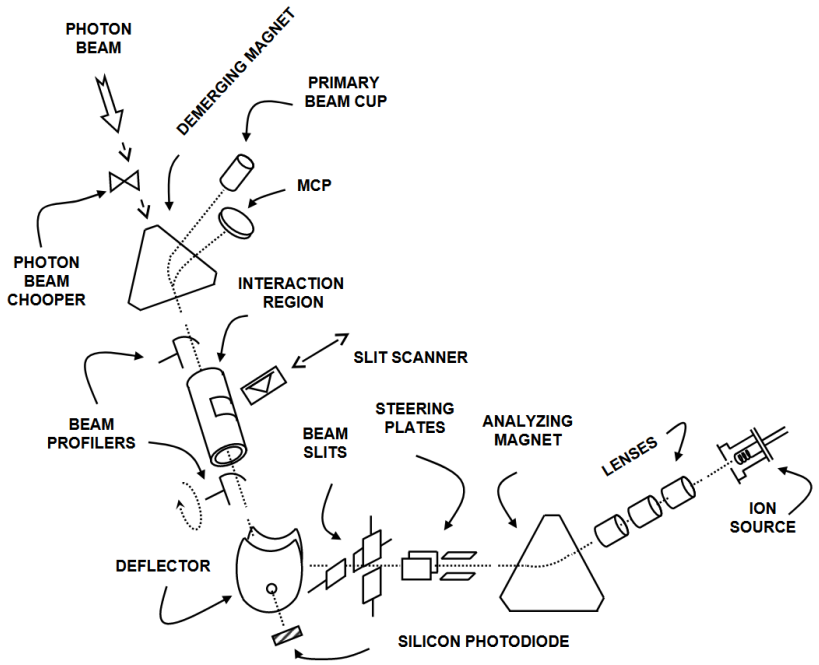

Figure 1. Schematic of the MBT end-station.

In this stage, the photon beam and the ion beam overlap, and as a consequence, photons can ionize the ion beam. Ions resulting from the overlapping will be called photo-ions. Photo-ions and the ion beam traveled through a voltage bias (typically, 2 kV) metallic mesh or interaction region. Photo-ions produced in this section, suffer a different electric field from those photo-ions produced outside, thereby defining a fixed interaction distance. In this manner, photo-ions produced in this region had a different energy and it was possible to separate them from the parent ion beam by a second analyzing magnet. The interaction region has entrance and exit apertures to help define an effective interaction length. The experiment operated under ultrahigh vacuum conditions.

Intensity distributions $I^{+}(x,y)$ of both beams were measured by rotating-wire beam profilers installed before and after the interaction region. A third beam profiler consisted of a mechanically translating-slit scanner positioned halfway between the interaction region.

A second analyzing magnet separated the X^{q+} ion beam from the $X^{(q+s)+}$ photo-ions. The parent ion beam was monitored by an elongated Faraday cup. The second magnetic field was adjusted such that the $X^{(q+s)+}$ photo-ions passed through an aperture in the back of the Faraday cup. A spherical 90° electrostatic deflector directed them onto a stainless steel plate biased at -550 V, from which secondary electrons were accelerated and detected by a microsphere-plate electron multiplier used in a pulse-counting mode.

The detector's planes were perpendicular to the beam trajectory, allowing the photo-ions be scanned across the detector, and verify full collection by measuring a plateau as a function of the pertinent parameters. The efficiency of the photo-ion detector was calibrated *in situ* using an averaging sub-femtoampere meter to record the $X^{(q+s)+}$ photo-ion current, which was then compared to the measured photo-ion count rate. The primary X^{q+} ion beam current was measured by a precision current meter.

The overlap of the photon and ion beams, in addition to the interaction region dimensions are needed to measure the cross-section. For this purpose, the beam intensity distributions measured with the beam profilers, $I^{+}(x,y)$ of the ion beam and $I^{\gamma}(x,y)$ of the photon beam, were measured, and a form factor $F(z)$ was derived according to,

Preprints (www.preprints.org) | NOT PEER-REVIEWED | Posted: 15 December 2023 doi:10.20944/preprints202312.1161.v1

$$F_i(z) = \frac{\int\int I^+(x,y)I^\gamma(x,y)dxdy}{\int\int I^+(x,y)dxdy \int\int I^\gamma(x,y)dxdy}\,, \tag{7}$$

where z is the axis assigned to the propagation direction of the ion beam. $F(z)$ was sampled at the three positions where profilers were mounted: the entrance, the center, and the exit of the interaction region. These values, $F_i(z)$, were used to derive $F(z)$ by interpolation along the total interaction region length and derive, by integration over z, the spatial overlap of the photon and ion beams the interaction region path [33].

The photoionization cross-section, σ, was derived from the experimental parameters as follows,

$$\sigma = \frac{Rqe^2v_i\epsilon}{I^+I^\gamma \int F(z)dz}\,, \tag{8}$$

where R is the photo-ion count rate, q is the charge state of X^{q+} parent-ion $e = 1.6 \times 10^{-19}$ C, v_i is the ion beam velocity in $cm \cdot s^{-1}$, ϵ is the responsivity of the photo-diode (electrons per photon), I^+ is the ion beam current (A), and I^γ is the photo-diode current (A).

Past Reviews on Measured Photoionization of Ions

We present a list of references for photoionization cross sections for various ions measured at ALS in Table 1. We discuss cross sections from other set-ups and the sources of information below.

There exists some reviews on the subject earlier measurements of photoionization cross sections. The review by Schmith in 1992 [36], presents a comprehensive treatment of both theory and experimentation with synchrotron radiation up to that date. There is still no reference to the merged-beam technique. It is a handy reference for general aspects and terminology of first principles theoretical methods. The Sonntag and Zimmermann review in 1992 [37] concentrates on PI experiments of metallic vapors with synchrotron radiation above 20 eV. It presents an interesting review of available techniques to that date, like He-discharge and lasers. The authors mentioned that R-matrix is a more convenient method to describe PI over extended energy regions.

In 2001 West's review [38] it is mentioned that there had been two main methods to measure photoionization spectra and cross sections, plasma discharge and merged beam technique. He brings forward that the first experimental measurements of photoionization cross sections were reported by Lyon and collaborators [39]. Up to the date of the review, the majority of measurements are concentrated in spectra measured with the plasma discharge method. A description of the plasma ionization technique evolution is presented. In this review, the merged beam technique is described to a good extent. This review emphasizes cases where both methods, plasma ionization and the merged beams technique have been complementary. It raises the fact that the amount of experimental data available to date was not comparable with the data generated by theory, to a certain degree, this statement is still valid. By 2006, Kjeldsen [40] covers the state of the art focused in MBT experimentation with synchrotron radiation. Finally, the photoionization of metal atoms is also reviewed by [41] and relevant to astrophysics PI data is reviewed by Schippers and Müller [42].

Preprints (www.preprints.org) | NOT PEER-REVIEWED | Posted: 15 December 2023 doi:10.20944/preprints202312.1161.v1

Table 1. Photoionization measurements of simple ions at the ALS.

Li II	$\longrightarrow$	Li III	S. W. J. Scully, *et al.*, J. Phys. B: At. Mol. Opt. Phys., **39**, 3957, 2006
B III	$\longrightarrow$	B IV	A. Müller, *et al.*, J. Phys. B: At. Mol. Opt. Phys., **43**, 135602, 2010
B II	$\longrightarrow$	B III	S. Schippers, *et al.*, J. Phys. B: At. Mol. Opt. Phys., **36**, 3371, 2003
B II	$\longrightarrow$	B III	A. Müller, *et al.*, J. Phys. B: At. Mol. Opt. Phys., **47**, 135201, 2014
C IV	$\longrightarrow$	C V	A. Müller, *et al.*, J. Phys. B: At. Mol. Opt. Phys., **42**, 235602, 2009
C III	$\longrightarrow$	C IV	A. Müller, *et al.*, Nucl. Instrum. Meth. B, **205**, 301, 2003
C III	$\longrightarrow$	C IV	S. W. J. Scully, *et al.*, J. Phys. B: At. Mol. Opt. Phys., **38**, 1967, 2005
C III	$\longrightarrow$	C IV	A. Müller, *et al.*, J. Phys. B: At. Mol. Opt. Phys., **35**, L137, 2002
C III, N IV, O V	$\longrightarrow$	C IV, N V, O VI	A. Müller, *et al.*, J. Phys. B: At. Mol. Opt. Phys., **43**, 225201, 2010
C II	$\longrightarrow$	C III	A. S. Schlachter, *et al.*, J. Phys. B: At. Mol. Opt. Phys., **37**, L103, 2004
O II	$\longrightarrow$	O III	A. M. Covington, *et al.*, Phys. Rev. Lett. **87**, 243002, 2001
O II	$\longrightarrow$	O III	A. Aguilar, *et al.*, ApJS **146**, 467, 2003
Ne IV, F III	$\longrightarrow$	Ne V, F IV	A. Aguilar, *et al.*, J. Phys. B: At. Mol. Opt. Phys., **38** 343, 2005
Ne III	$\longrightarrow$	Ne IV	S. N. Nahar, *et al.*, Int. J. Mass Spectrom., **443**, 61-69, 2019
Ne II	$\longrightarrow$	Ne III	A. M. Covington, *et al.*, Phys. Rev. A **66**, 062710, 2002
Na^-	$\longrightarrow$	Na^+	A. M. Covington, *et al.*, J. Phys. B: At. Mol. Opt. Phys., **34** L735, 2001
Mg II, Al III	$\longrightarrow$	Mg III, Al IV	A. Aguilar, *et al.*, Phys. Rev. A, **67**, 012701, 2003
Al II	$\longrightarrow$	Al III	C. E. Hudson, *et al.*, J. Phys. B: At. Mol. Opt. Phys., **38**, 2911, 2005
CO^+	$\longrightarrow$	CO^{2+}	G. Hinojosa, *et al.*, Phys. Rev. A, **66**, 032718, 2002
CO^+	$\longrightarrow$	O^+	G. Hinojosa, *et al.*, J. Phys. B: At. Mol. Opt. Phys., **38**, 2701, 2005
P III, P IV	$\longrightarrow$	P IV, P V	L. Hernández, *et al.*, J. Quant. Spectroc. Ra., **159**, 80-86, 2015
P II	$\longrightarrow$	P III	S. N. Nahar, *et al.*, **187**, 215-223, 2017
Cl III	$\longrightarrow$	Cl IV	S. N. Nahar, *et al.*, Atoms, **11**, 28, 2023
Cl II	$\longrightarrow$	Cl III	E. M. Hernández, *et al.*, J. Quant. Spectroc. Ra., **151**, 217, 2015
Ar VI	$\longrightarrow$	Ar VII	Jing Cheng Wang, *et al.*, Phys. Rev. A, **75**, 062712, 2007
Ar II	$\longrightarrow$	Ar III	A. M. Covington, *et al.*, Phys. Rev. A **84**, 013413, 2011
Ar II	$\longrightarrow$	Ar IV	A. Müller, *et al.*, Phys. Rev. A, **103**, L031101, 2021
K III	$\longrightarrow$	K IV	G. A. Alna'Washi, *et al.*, Phys. Rev. A, **90**, 023417 , 2014
Ca IV	$\longrightarrow$	Ca V	Ghassan A. Alna'washi, *et al.*, Phys. Rev. A, **81**, 053416, 2010
Ca II	$\longrightarrow$	Ca III	A. Müller, *et al.*, J. Phys. B: At. Mol. Opt. Phys., **50**, 205001, 2017
Sc III	$\longrightarrow$	Sc IV	S. Schippers, *et al.*, Phys. Rev. Lett., **89**, 193002, 2002
Sc III	$\longrightarrow$	Sc IV	S. Schippers, *et al.*, Phys. Rev. A, **67**, 032702, 2003
Sc III	$\longrightarrow$	Sc IV	S. Schippers, *et al.*, Nucl. Instrum. Meth. B, **205**, 297, 2003
Ti IV	$\longrightarrow$	Ti V	S. Schippers, *et al.*, 2004, J. Phys. B: At. Mol. Opt. Phys., **37**, L209
Fe IV, VI, VIII	$\longrightarrow$	Fe V, VII, IX	M. F. Gharaibeh, *et al.*, Phys. Rev. A, **83**, 043412, 2011
Zn II	$\longrightarrow$	Zn III	G. Hinojosa, *et al.*, Mon. Not. R. Astron. Soc., **470**, 4048-4060, 2017
Se IV, Se VI	$\longrightarrow$	Se V, Se VII	D. A. Esteves, *et al.*, J. Phys. B: At. Mol. Opt. Phys., **45**, 115201, 2012
Se III	$\longrightarrow$	Se IV	D. A. Macaluso, *et al.*, Phys. Rev. A, **92**, 063424, 2015
Se II	$\longrightarrow$	Se III	N. C. Sterling, *et al.*, J. Phys. B: At. Mol. Opt. Phys., **44**, 025701, 2011
Se II	$\longrightarrow$	Se III	D. A. Esteves, *et al.*, Phys. Rev. A, **84**, 013406, 2011
Kr VI	$\longrightarrow$	Kr VII	M. Lu, *et al.*, Phys. Rev. A. **74**, 012703, 2006
Kr IV	$\longrightarrow$	Kr V	M. Lu, *et al.*, Phys. Rev. A, **74**, 062701, 2006
Kr II	$\longrightarrow$	Kr III	G. Hinojosa, *et al.*, Phys. Rev. A, **86**, 063402, 2012
Xe V- VII	$\longrightarrow$	Xe VI- VIII	A. Aguilar, *et al.*, Phys. Rev. A, **73**, 032717, 2006
Xe IV	$\longrightarrow$	Xe V	E. D. Emmons, *et al.*, Phys. Rev. A, **71**, 042704, 2005
Xe VIII	$\longrightarrow$	Xe IX	A Müller, *et al.*, J. Phys. B: At. Mol. Opt. Phys., **47**, 215202, 2014
W VI	$\longrightarrow$	W VII	A. Müller, *et al.*, J. Phys. B: At. Mol. Opt. Phys., **52**, 195005, 2019
W V	$\longrightarrow$	W VI	A. Müller, *et al.*, J. Phys. B: At. Mol. Opt. Phys., **50**, 085007, 2017
W III- IV	$\longrightarrow$	W IV- V	B. M. McLaughlin, *et al.*, J. Phys. B: At. Mol. Opt. Phys., **49**, 065201, 2016
W II, IV, VI	$\longrightarrow$	W III, V, VII	A. Müller, *et al.*, Phys. Scr., **T144**, 014052, 2011
W II	$\longrightarrow$	W III	A. Müller, *et al.*, J. Phys. B: At. Mol. Opt. Phys., **48**, 235203, 2015
Ce III - Ce V	$\longrightarrow$	Ce IV - Ce VI	A. Müller, *et al.*, Phys. Rev. Lett., **101**, 133001, 2008
Ce II - Ce X	$\longrightarrow$	Ce III - Ce XI	M. Habibi, *et al.*, Phys. Rev. A, **80**, 033407, 2009

4. New Additions to NORAD-Atomic-Data

The database NORAD-Atomic-Data has been enhanced by additions of new data, as described below, of atomic processes.

Preprints (www.preprints.org) | NOT PEER-REVIEWED | Posted: 15 December 2023 doi:10.20944/preprints202312.1161.v1

1.) Among the data added, a signiicant amount of new data is related to spectral formation from photo-excitation cross sections of atoms and ions. There are of three types of such data. i) Atomic data for x-ray spectroscopy, especially for K-α and K-β transitions for resonance fluorescence effect predicted by Pradhan et al [43] for biomedical applications and was later observed experimentally [44] as shown in Figure 1. ii) Photoiexcitation data for spectral formation by ions of bio-signature elements, such as phosphorus, e.g. [46]. iii) Atomic data for spectroscopy of lanthanides of neutral to low ionization stages which may relate to the electromagnetic waves created during a kilonovae event of merger of two neutron stars or black holes, e.g. [47].

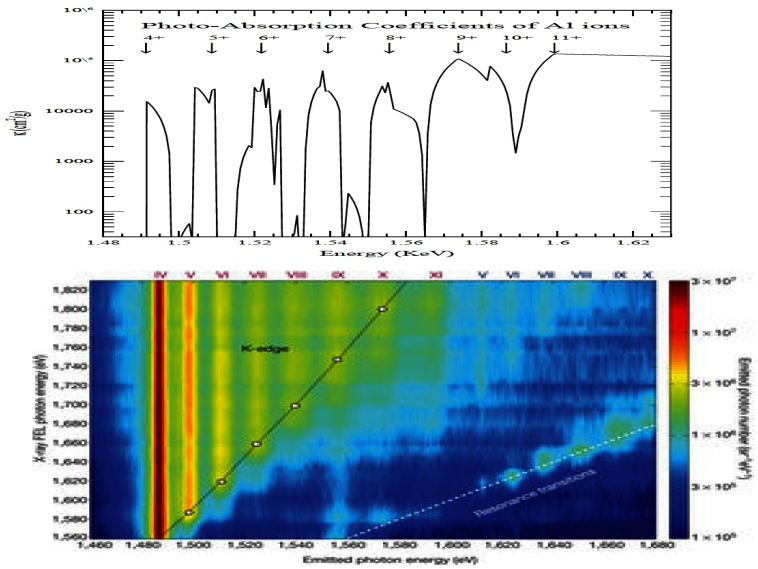

Figure 2. K_α resonance fluorescence in Al plasma [44]. Top: Theoretically computed K_α absorption features in Al ions isoelectronic with F to He are shown (ionization states are labeled in the top panel and roman numerals in the bottom panel). All contributing K_α transition strengths are added together and shown in terms of X-ray attenuation coefficients (cm2/g) (convoluted over a Gaussian FWHM of 10 eV). Bottom: Experimental measurements from the LCLS-XFEL [45] (reproduced with permission). The dashed line on the right shows the resonance transitions with increasing K_α emission intensity corresponding to the theoretical absorption complexes. The observed K_α features appear when the XFEL energy equals the emitted photon energy.

2.) The second addition is inclusion of collisional data for collision strengths and rate coefficients for electron impact excitation (EIE). NORAD-Atomic-Data considered almost no collisional data in the past since these data for various atomic systems are available from TIPbase [8] and from other investigators. However, for possible plasma diagnostics, NORAD-Atomic-Data has started to include these collisional data, e.g. for Ca IV [48].

3.) The the third addition is the inclusion of experimental data for energy levels, oscillator strengths. NIST database [16] is the main source for compiled and evaluated experimental oscillator strengths and radiative decay rates. We have added large sets of experimental energy levels and transition parameters of a number of heavy ions, obtained mainly from the leading spectroscopy laboratory of Aligarh Muslim University in India. These files contain complete sets of transitions that were measured in comparison to the evaluated sets available at NIST. The added data are currently for eight ions, Ag III [49], Ag-IV [50], Au V [55], Bi IV [52], Hg III [53], Hg-IV [54], Hg V [55], Hg-VI [55]. For the transition parameters, they used vacuum spectrograph for measurement of spectral lines from exposures created by discharge of electrodes, containing the sample, with a trigger module of high voltage electrical pulse. Details of their experiments, calibration and analysis are given in their papers.

Preprints (www.preprints.org) | NOT PEER-REVIEWED | Posted: 15 December 2023 doi:10.20944/preprints202312.1161.v1

Aligarh lab has produced spectral data for many ions. However, currently available data are largely in pdf-formatted files which were saved with publications. More data will be added to NORAD-Atomic-Data when the authors provide the data files converted to ASCII formatted files.

4.) The fourth addition is the inclusion of experimental data for photoionization cross sections. Most experimental set-ups are typically synchrotron based, such as, Advanced Light Source (ALS) of synchrotron at Lawrence Berkeley National Lab (LBNL), set-ups at University of Paris-SUD, Aahus University, BESSY and PETRA in Germany. Another set-up used is laser-induced excited state photoionization in Pakistan and University of Nebraska. Among the experimental photoionization cross section data for ions available at NORAD-Atomic-Data are Cl III [56], Cl II [57], K [58], etc.

5.) The fifth addition of NORAD-Atomic-Data is a web-based interactive feature to obtain line ratios for plasma diagnostics. NORAD-Atomic-Data has all the basic radiative, except for the collisional data for EIE, to calculate the line ratio diagnostics for many atoms and ions. Our recent study on line ratios of P II [59], with inclusion of electron-ion recombination cascade effect which was known to have impact not considered in the astrophysical models before, demonstrated that the effect can lower or increase the line ratios. Figure 3 presents an exemplary impact of electron-ion recombination on line ratios (red) curve compared to that without the effect (dark red) on the low lying transitions in P II [59].

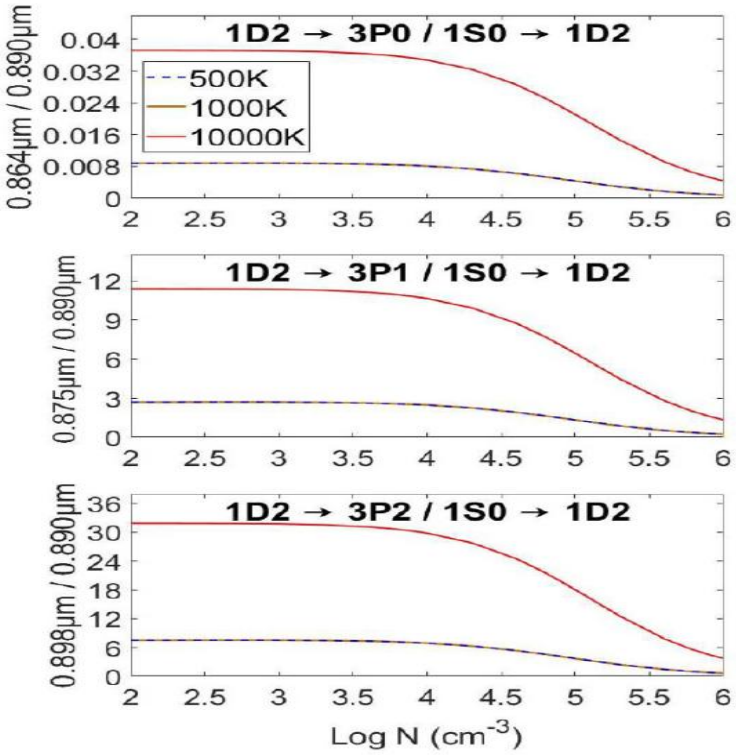

Figure 3. Emissivity ratios of [P II] lines at ionospheric and nebular temperatures 500K, 1000K, and 10,000K lying within and potentially observed by by JWST spectrometers. While 500K and 1000 K lines (dark red) appear to be identical, they differ by a few percentage points at all, far less than the difference from the 10,000 K line [59].

We have computed the relevant atomic quantities in large sets that can used to compute the line ratios for diagnostics over a large range temperatures and densities. A preliminary version of the code is in operaturation at the the web-based interactive feature for computing the line ratios at any temperature and density.

Preprints (www.preprints.org) | NOT PEER-REVIEWED | Posted: 15 December 2023 doi:10.20944/preprints202312.1161.v1

5. Conclusions

An overview with general outlines of contents on the new additions to database NORAD-Atomic-Data is presented. There are six additions that have been discussed for the expansion of the database. Significant enhancements of data are due to additions of experimental data, not included before, and data for photo-absorption spectral features.

Testing of data for accuracy is given a high priority. Majority of data have been obtained from ab initio R-matrix method. Results using atomic structure calculations have also been added for cases they provide good accuracy, such as for x-ray or high energy region where perturbations and electron-electron interactions are relatively negligible, and for cases, such as large data need for large atomic systems of lanthanides where numerical extends are prohibitive for R-matrix codes.

While theoretical overview along with description of data, accuracy and benchmarking of the online database were presented in the earlier paper on the database [1], here we present general overview of experimental background, particularly of photoionization.

Future direction are:

i) include more data, both radiative and collisional, with publications

ii) include computer programs that can read the data files and process the data to calculate the quantities of interest

iii) add more data for the web-based feature to compute spectral line ratios of other atoms and ions for astrophysical applications,

iv) an option for selection of partial data, such as, for a particular wavelength range

Author Contributions: S.N. Nahar and Guillermo Hinojosa have written up the article together.

Funding: This research had computational support from Ohio Supercomputer Center (SNN). GH acknowledges funding from CONAHCyT CF-2023-I-918 in Mexico.

Acknowledgments: Nahar acknowledges use of high performance computers at Ohio Supercomputer Center.

Conflicts of Interest: The authors declare no conflict of interest.

References

1. 'Database NORAD-Atomic-Data for atomic processes in plasma", Sultana N. Nahar, Atoms 8, issue 4, 68 (2020), DOI 10.3390/atoms8040068
2. Nahar SN, NaharOSURadiative(NORAD)-Atomic-Data at url:http://norad.astronomy.osu.edu/, The Ohio State University (2007)
3. Seaton MJ .Atomic data for opacity calculations. I. General description. *J. Phys. B* **1987** *20*, 6363-6378
4. *The Opacity Project*, The Opacity Project Team, Institute of Physics Publishing, Vol. 1 (1995), Vol. 2(1996)
5. Hummer DG, Berrington KA, Eissner W, Pradhan AK, Saraph HE, Tully JA .Atomic data from the IRON Project. 1: Goals and methods. *Astron. Astrophys.* **1993**; *279*, 298-309
6. Cunto W, Mendoza C, Ochsenbein F and Zeippen C J. .TOPbase at the CDS. *Astron. Astrophys.* **1993**, *275*, L5-8
7. TOPbase: http://cdsweb.u-strasbg.fr/topbase/topbase.html (1992)
8. TIPbase: http://cdsweb.u-strasbg.fr/tipbase/home.html (2001)
9. Pradhan A.K., Nahar S.N. *Atomic Astrophysics and Spectroscopy* (Cambridge University Press, 2011)
10. Berrington, K.A., Burke, P.G., Butler, K., Seaton, M.J., Storey, P.J., Taylor, K.T., Yan, Yu. .Atomic data for opacity calculations. II. Computational methods. *J. Phys. B* **1987** *20*, 6379-6397
11. S.N. Nahar, "Atomic Data from the Iron Project VII. Radiative dipole transition probabilities for Fe II" (ELEVID), Astron.Astrophys. 293, 967-977 (1995)
12. S.N. Nahar "Fine structure transitions in Fe XIV" (PRCBPID), New Ast 21 (2013) 8–16
13. Berrington, K.A., Eissner, W., Norrington, P.H. .RMATRIX1: Belfast atomic R-matrix codes. *Comput. Phys. Commun.* **1995** *92*, 290-420
14. Eissner W, Jones M, Nussbaumer H .Techniques for the calculation of atomic structures and radiative data including relativistic corrections. *Comput. Phys. Commun.* **1974**, *8*, 270-306

Preprints (www.preprints.org) | NOT PEER-REVIEWED | Posted: 15 December 2023 doi:10.20944/preprints202312.1161.v1

15. Nahar SN, Eissner W, Chen GX, Pradhan AK. Atomic data from the Iron Project - LIII. Relativistic allowed and forbidden transitionstic probabilities for Fe XVII. *Astron. Astrophys.* **2003**, *408*, 789-8016
16. NIST: https://physics.nist.gov/PhysRefData/ASD/levels_form.html
17. Nahar S.N., Pradhan A.K. .Unified Treatment of Electron-Ion Recombination in the Close Coupling Approximation. *Phys. Rev. A* **1994**, *49*, 1816
18. Zhang H.L., Nahar SN, Pradhan, AK .Close coupling R-matrix calculations for electron-ion recombination cross sections. *J. Phys. B* **1999**, *32*, 1459-1479
19. Nahar SN, Pradhan AK .Electron-ion recombination in the close coupling approximation. *Phys. Rev. Lett.* **1992**, *68*, 1488-1491
20. Bell RH, Seaton MJ. Dielectronic recombination: I. General theory. *J. Phys. B* **1985**, *18*, 1589-1629
21. Phaneuf, R.A.; Havener, C.C.; Dunn, G.H.; Müller, A. Merged-beams experiments in atomic and molecular physics. Rep. Prog. Phys. 1999, 62, 1143. https://doi.org/10.1088/0034-4885/62/7/202.
22. G, M. Synchrotron light: A success story over six decades. Riv. Nuovo Cimento 2017, 40, 411–471. https://doi.org/10.1393/ncr/i2017-10139-3.
23. Müller, A.; Schippers, S.; Hellhund, J.; Holste, K.; Kilcoyne, A.L.D.; Phaneuf, R.A.; Ballance, C.P.; McLaughlin, B.M. Single-photon single ionization of W+ ions: experiment and theory. J. Phys. B: At., Mol. Opt. Phys. 2015, 48, 235203. https://doi.org/10.1088/0953-4075/48/23/235203.
24. Nahar, S.N.; Hernández, E.M.; Kilcoyne, D.; Antillón, A.; Covington, A.M.; González-Magaña, O.; Hernández, L.; Davis, V.; Calabrese, D.; Morales-Mori, A.; et al. Experimental and Theoretical Study of Photoionization of Cl III. Atoms 2023, 11. https://doi.org/10.3390/atoms11020028.
25. Esteves, D.A.; Bilodeau, R.C.; Sterling, N.C.; Phaneuf, R.A.; Kilcoyne, A.L.D.; Red, E.C.; Aguilar, A. Absolute high-resolution Se+ photoionization cross-section measurements with Rydberg- series analysis. Phys. Rev. A 2011, 84, 013406. https://doi.org/10.1103/PhysRevA.84.013406.
26. Domke, M.; Schulz, K.; Remmers, G.; Kaindl, G.; Wintgen, D. High-resolution study of 1 P0 double-excitation states in helium. Phys. Rev. A 1996, 53, 1424–1438. https://doi.org/10.1103/PhysRevA.53.1424.
27. King, G.C.; Tronc, M.; Read, F.H.; Bradford, R.C. An investigation of the structure near the L2,3 edges of argon, the M4,5 edges of kryton and the N4,5 edges of xenon, using electron impact with high resolution. J. Phys. B-At. Mol. Opt. 1977, 10, 2479–2495. https://doi.org/10.1088/00 22-3700/10/12/026.
28. Hernández, E.; Juárez, A.; Kilcoyne, A.; Aguilar, A.; Hernández, L.; Antillón, A.; Macaluso, D.; Morales-Mori, A.; na, O.G.M.; Hanstorp, D.; et al. Absolute measurements of chlorine Cl+ cation single photoionization cross section. Journal of Quantitative Spectroscopy and Radiative Transfer 2015, 151, 217–223. https://doi.org/10.1016/j.jqsrt.2014.10.004.
29. Kramida, A.; Yu. Ralchenko.; Reader, J.; and NIST ASD Team (2022). NIST Atomic Spectra Database (ver. 5.10), [Online]. Available: http://physics.nist.gov/asd [2014, February 25]. National Institute of Standards and Technology, Gaithersburg, MD., 2022. https://doi.org/https: //doi.org/10.18434/T4W30F.
30. Lu, M.; Gharaibeh, M.F.; Alna'washi, G.; Phaneuf, R.A.; Kilcoyne, A.L.D.; Levenson, E.; Schlachter, A.S.; Müller, A.; Schippers, S.; Jacobi, J.; et al. Photoionization and electron- impact ionization of Kr5+ . Phys. Rev. A 2006, 74, 012703. https://doi.org/10.1103/PhysRevA.74.012703.
31. Müller, A.; Schippers, S.; Phaneuf, R.A.; Kilcoyne, A.L.D.; Bräuning, H.; Schlachter, A.S.; Lu, M.; McLaughlin, B.M. State-resolved valence shell photoionization of Be-like ions: experiment and theory. J. Phys. B: At., Mol. Opt. Phys. 2010, 43, 225201. https://doi.org/10.1088/0953-4075/43/22/225201.
32. Covington, A.M.; Aguilar, A.; Covington, I.R.; Gharaibeh, M.; Shirley, C.A.; Phaneuf, R.A.; Alvarez, I.; Cisneros, C.; Hinojosa, G.; Bozek, J.D.; et al. Photoionization of Metastable O+ Ions: Experiment and Theory. Phys. Rev. Lett. 2001, 87, 243002. https://doi.org/10.1103/ PhysRevLett.87.243002.
33. Covington.; Aguilar, A.M.; A. Covington, I.R.; Gharaibeh, M.F.; Hinojosa, G.; Shirley, C.A.; Phaneuf, R.A.; Alvarez, I.; Cisneros, C.; Dominguez-Lopez, I.; et al. Photoionization of Ne+ using synchrotron radiation. Phys. Rev. A 2002, 66, 062710. https://doi.org/10.1103/PhysRevA. 66.062710.
34. Covington, A.M.; Aguilar, A.; Davis, V.T.; Alvarez, I.; Bryant, H.C.; Cisneros, C.; Halka, M.; Hanstorp, D.; Hinojosa, G.; Schlachter, A.S.; et al. Correlated processes in inner-shell photodetachment of the Na- ion". Journal of Physics B: Atomic, Molecular and Optical Physics 2001, 34, L735. https://doi.org/10.1088/0953-4075/34/22/105.
35. Scully, S.W.J.; Alvarez, I.; Cisneros, C.; Emmons, E.D.; Gharaibeh, M.F.; Leitner, D.; Lubell, M.S.; Müller, A.; Phaneuf, R.A.; Püttner, R.; et al. Doubly excited resonances in the photoionization

Preprints (www.preprints.org) | NOT PEER-REVIEWED | Posted: 15 December 2023 doi:10.20944/preprints202312.1161.v1

spectrum of Li + : experiment and theory. J. Phys. B: At., Mol. Opt. Phys. 2006, 39, 3957. https://doi.org/10.1088/0953-4075/39/18/024.
36. Schmidt, V. Photoionization of atoms using synchrotron radiation. Rep. Prog. Phys. 1992, 55, 1483. https://doi.org/10.1088/0034-4885/55/9/003.
37. Sonntag, B.; Zimmermann, P. XUV spectroscopy of metal atoms. Rep. Prog. Phys. 1992, 55, 911. https://doi.org/10.1088/0034-4885/55/7/002.
38. West, J.B. Photoionization of atomic ions. J. Phys. B-At. Mol. Opt. 2001, 34, R45. https://doi.org/10.1088/0953-4075/34/18/201.
39. Lyon, I.C.; Peart, B.; West, J.B.; Dolder, K. Measurements of absolute cross sections for the photoionisation of Ba+ ions. J. Phys. B-At. Mol. Opt. 1986, 19, 4137. https://doi.org/10.1088/0022-3700/19/24/015.
40. Kjeldsen, H. Photoionization cross sections of atomic ions from merged-beam experiments. J. Phys. B- At. Mol. Opt. 2006, 39, R325. https://doi.org/10.1088/0953-4075/39/21/R01.
41. Martins, M.; Godehusen, K.; Richter, T.; Wernet, P.; Zimmermann, P. Open shells and multi- electron interactions: core level photoionization of the 3d metal atoms. J. Phys. B-At. Mol. Opt. 2006, 39, R79. https://doi.org/10.1088/0953-4075/39/5/R01.
42. Schippers, S.; Müller, A. Photoionization of Astrophysically Relevant Atomic Ions at PIPE. Atoms 2020, 8, 45. https://doi.org/doi:10.3390/atoms8030045.
43. "Resonant X-Ray Enhancement of the Auger Effect in High-Z atoms, molecules, and Nanoparticles: Biomedical Applications", A.K. Pradhan, S.N. Nahar, M. Montenegro, Y. Yu, H.L. Hang, C. Sur, M. Mrozik, R. Pitzer, J. Phys. Chem. A 113, 12356-12363 (2009)
44. "K_α resonance fluorescence in Al, Ti, Cu and potential applications for X-ray sources", Sultana N. Nahar and Anil K. Pradhan, JQSRT 155, 32-48 (2015)
45. Vinko SM, Ciricosta O, Cho BI, Engelhorn K, Chung H-K, Brown CRD et al. .Creation and diagnosis of a solid-density plasma with an X-ray free-electron laser. Nature 2012;482:59-62
46. "Spectra of phosphorus ions for astrophysical modeling: P I - P XV:, S.N. Nahar and B. Shafique (submitted 2023)
47. "Theoretical spectra of lanthanides for kilonovae events: Ho I-III, Er I-IV, Tm I-V, Yb I-VI, Lu I-VII", S.N. Nahar (submitted 2023)
48. "Collisional- and photo-excitations of Ca IV including strong3.2 μm emission line", Sultana N. Nahar and Bilal Shafique, Eur. Phys. J. D 77, 45- (11 pages, 2023, https://doi.org/10.1140/epjd/s10053-023-00622-8)
49. "Revised and extended analysis of the third spectrum of silver: Ag III", S. Ankita and A. Tauheed, J. Quant. Spectros. Rad. Transfer 217, 130-154 (2018)
50. "Spectral analysis of triply ionized silver (Ag IV)", S. Ankita, A. Tauheed, J. Quant. Spectros. Rad. Transfer 254, 107193 (2020)
51. "Energy structure and radiative parameter calculations in the Re-like Pt IV, Au V and Hg VI spectra and preliminary line identifications in Hg VI.", A. Tauheed and Aadil Rashid, J. Quant. Spectrosc. Radiat. Transfer. 261 (2021) 107435
52. "Energy levels, wavelengths and radiative rates for transitions in Hg-like Bismuth", Neelam Kumari Arya, A. Tauheed, J. Quant. Spectros. Rad. Transfer 292, 108353 (2022)(doi: https://doi.org/10.1016/j.jqsrt.2022.108353)
53. "Revised analysis of doubly ionized mercury: Hg III-3" Aadil Rashid and A. Tauheed, J. Quant. Spectrosc. Radiat. Transfer. 233 (2019) 119-33
54. "Energy structure investigations in triply ionized mercury: Hg IV", Aadil Rashid and A. Tauheed, J. Quant. Spectrosc. Radiat. Transfer. 270 (2021) 107668
55. "Energy structure and radiative parameter calculations in the Re-like Pt IV, Au V and Hg VI spectra and preliminary line identifications in Hg VI.", A. Tauheed and Aadil Rashid, J. Quant. Spectrosc. Radiat. Transfer. 261 (2021) 107435
56. S.N. Nahar, E.M. Hernández, D. Kilkoyne, A. Antillón, A.M. Covington, O. González-Magaña, L. Hernández, V. Davis, D. Calabrese, A. Morales-Mori, D. Hanstorp, A. M. Juárez and Guillermo Hinojosa., Atoms, Vol. 11, page 28 (2023). https://doi.org/10.3390/atoms11020028
57. "Absolute measurements of chlorine Cl+ cation single photoionization cross section", E. M. Hernández, A. M. Juárez, A. L. D. Kilcoyne, A. Aguilar, L. Hernández, A. Antillón, D. Macaluso, A. Morales-Mori, O. González-Magaña, D. Hanstorp, A. M. Covington, V. Davis, D. Calabrese, G.

Preprints (www.preprints.org) | NOT PEER-REVIEWED | Posted: 15 December 2023 doi:10.20944/preprints202312.1161.v1

Hinojosa. Journal of Quantitative Spectroscopy and Radiative Transfer, Vol. 151, p217-223 (2015). http://dx.doi.org/10.1016/j.jqsrt.2014.10.004

58. Valence-shell single photoionization of Kr+ ions: Experiment and theory. G. Hinojosa, A. M. Covington, G. A. Alna-Washi, M. Lu, R. A. Phaneuf M. M. Sant-Anna, C. Cisneros, I. Alvarez, Aguilar, A. L. D. Kilcoyne, A. S. Schlachter, C. P. Ballance, B. M. McLaughlin. Phys Rev A 86, 063402 (2012) DOI: 10.1103/PhysRevA.86.063402 https://journals.aps.org/pra/abstract/10.1103/PhysRevA.86.063402
59. K. Hoy, S.N. Nahar, A.K. Pradhan, Mon. Not. R. Soc "Biosignature Line Ratios of [P II] in Exoplanetary andNebular Environments", Kevin Hoy, Sultana N. Nahar, Anil K. Pradhan, MNRAS Lett 521, L48-L52 (2023),

Disclaimer/Publisher's Note: The statements, opinions and data contained in all publications are solely those of the individual author(s) and contributor(s) and not of MDPI and/or the editor(s). MDPI and/or the editor(s) disclaim responsibility for any injury to people or property resulting from any ideas, methods, instructions or products referred to in the content.